Nanoscratch profiles of hybrid films based on (3-glycidoxypropyl)trimethoxysilane and modified with tetraethoxysilane

L. Hu*, X. Zhang and Y. Huang

Silsesquioxanes (SSO) derived from the hydrolytic condensation of (3-glycidoxypropyl)trimethoxysilane (GPMS) and tetraethoxysilane (TEOS) were prepared by the sol–gel process. Hardness *H* and elastic modulus *E* of the SSO films modified with 5, 10, 15, 20, 25 and 30 wt-%TEOS contents were measured by the continuous stiffness measurement technique and the brittle index *H/E* for the films was calculated from the results. The nanoscratch testing was carried out to study the influence of the different TEOS contents of the coatings on the scratch-testing profiles, including the pre-scan, scratch-scan and post-scan profiles. The film containing 20 wt-%TEOS was found to have the best elastoplastic behaviour and scratch resistance, based on considerations including the baseline of the pre-scan profile, the depth of the scratch, the abrupt change in the scratching curve and the fluctuation and recovering characteristic for the post-scan profile.

Keywords: Silsesquioxanes, (3-Glycidoxypropyl)trimethoxysilane, Tetraethoxysilane, Sol–gel process, Nanoindentation, Nanoscratch, Coefficient of friction

Introduction

Studies in nanoscience generally involve polyhedral oligomeric silsesquioxanes (POSS) or organically modified silicates (Ormosils).[1,2] When these hybrid materials are applied as coatings on substrates, the usual requirement is to enhance the abrasion or scratch resistance.[3] In recent years, a nanoscratch testing using the continuous stiffness measurement (CSM) technique of the instrumented indentation testing (IIT)[4,5] and measurement with atomic force microscopy (AFM)[6,7] have been commonly used to characterize materials for scratch resistance, in preference to other techniques such as the microwedge scratch test (MWST) or scratch tests in macroscopic experiments.[8,9] In a CSM scratch test, a sharp tip is moved over the surface of the test material at a constant or ramp-up load. The load is ramped up until substantial damage occurs. Scratch depth at a given load or the load at which material fails catastrophically is a measure of scratch resistance. The coefficient of friction is also monitored during scratching. A typical scratch experiment consists of three steps: (1) approaching the surface (pre-scan), (2) translating the sample at ramping loads (scratch-scan) and (3) final unloading of the tip (post-scan).[10,11] Scratch-induced damage is monitored by *in situ* tangential (friction) force measurements and by light optical microscopy (LOM) imaging of the scratches after tests.[12,13]

Previous work on the nano-scratch test for thin films includes that by Roche *et al.*,[14] who studied various UV-cured clearcoats, applied on three different substrates (namely glass, aluminium and polycarbonate) at different layer thickness by both nanoindentation and nanoscratch techniques, and clearly illustrated the effects of soft and hard substrates on the indentation and scratch behaviours. Charitidis and coworkers[15] investigated the scratch performance of BN_x and CN_x films deposited onto Si(100) to evaluate the scratch resistance and the friction coefficient of the films, used as thin protective films on transparent antireflective coatings. Huang *et al.*[16,17] studied the wear and abrasion behaviour of particles on Ti-6Al-4V and Ti alloy substrates coated with diamond-like carbon (DLC) by fretting wear and nanoscratch test, and analyzed three regimes of the nanoscratch performance under loads of 200 and 400 mN, based on differences in the appearance of the scratch profile. Lemoine *et al.*[18] reported nano-indentation and scratch testing on magnetic recording tape heads coated with amorphous carbon layers less than 20 nm thick and found the limitation of the accuracy of the measurements was caused by the significant surface roughness of the samples. Conry *et al.*[19] investigated the nanoscratch technique to estimate hardness of ultrathin films when substrate effects were encountered with the nanoindentation technique, demonstrating that the nanoscratch method yielded the same hardness values as the nanoindentation method for homogeneous materials without surface layers. Martin's group[20] examined the mechanical properties and deformation mechanism of biocompatible protein thin films by scratch testing. In previous

Department of Applied Chemistry, Harbin Institute of Technology, Box 713, Harbin 150001, China

*Corresponding author, email hulijiang@vip.sina.com

Published by Maney on behalf of the Institute
Received 25 May 2004; accepted 17 March 2005
DOI 10.1179/174328904X48505

work,[21] the synthesis and characterization of silsesquioxane (SSO) obtained from the hydrolytic condensations of (3-glycidoxypropyl)trimethoxysilane (GPMS), and the mechanical properties (hardness and elastic modulus) of the GPMS–SSO films by the nanoindentation technique was reported. In this work, the focus is on the effect of the modifier contents on the nanoscratch performance for the GPMS–SSO films modified with tetraethoxysilane (TEOS).

For enhancing abrasion or scratch resistance, an increase in hardness is required, while a convenient low value of the brittle index, defined as the ratio of hardness to Young modulus, should be kept. Hardness can be increased by the addition of colloidal silica or TEOS to the initial formulation,[22] resulting in a much more rigid structure. However, this also results in an increase in brittleness. The optimum amount of silica to obtain a hard and tough coating is another interesting subject for the abrasion and scratch resistance.[23] In this work, the aim is to determine whether abrasion and scratch resistance could be improved by varying the amount of TEOS added.

Experimental

Materials

Commercial (3-glycidoxypropyl)trimethoxysilane (GPMS, Dow Corning Z-6030) was used in the study of hydrolytic condensation reactions. Ethanol (purity 99·7%) was used as solvent. Formic acid (88 wt-%) was employed as a catalyst, ethylenediamine (EDA), an analytical grade reagent, was chosen as a hardener for the curing process to form coatings, and tetraethoxysilane (TEOS, Aldrich) was employed as a modifier.

Sol–gel preparation

For the hydrolytic condensation reaction, GPMS and 5 to 30 wt-%TEOS were placed in a beaker. Ethanol was added to give a 3:1 molar ratio with respect to Si. The polycondensation was carried out in the presence of formic acid, added in a 3:1 molar ratio with respect to Si. Reactions taking place in the presence of formic acid have been described previously.[24] The beaker was sealed with a plastic film and the left for 3 days at 35°C. Then, needle-size holes were made in the plastic film and the reaction was continued for another 3 days at the same temperature. Finally, the plastic film was removed and the reaction continued for another 7 days at 35°C.

Coatings on glass substrates

First, the resulting TEOS-modified SSO derived from the hydrolytic condensation of GPMS was diluted with ethanol in a weight ratio 1:30 and EDA was then added to the solution. The amount of EDA added to the diluted SSO was determined as that giving the maximum glass transition temperature of the cured product. Second, dip-coating was performed on glass substrates (76·4 mm × 25·2 mm × 1·2 mm), at 270 mm min^{-1}. Finally, the coated glasses were cured in an oven at 80°C for 6 h, then for 2 h at 120°C. Coatings based on GPMS modified with TEOS will be denoted as GST (GPMS–SSO–TEOS). The thickness of the GST, 10 μm, was determined by scanning electron microscopy (SEM, Hitachi S-570).

Nanoindentation and nanoscratch testing

The hardness and elastic modulus of the coating systems were determined using a Nano Indenter XP (MTS Systems Corporation) device, incorporating the CSM technique. A triangular pyramid Berkovich indenter was used to fabricate the tip radius. Its indent shape and side view angles were 65·3° and 12·95°, respectively. The Poisson's ratio was 0·3; both the harmonic frame stiffness and the frame stiffness correction were 0 N m^{-1}, the loading rate $\bar{P}/P$ was 0·05 s^{-1} and the unload in stiffness calculation was 50%. Tests were performed in a clean-air environment with a relative humidity of approximately 30%, while the temperature was constantly kept at 23 ± 0·5°C. Equations used to determine hardness and elastic modulus from the experimental data are available in the literature.[4,25]

Scratch testing was measured by the NanoIndenter XP system with options for lateral-force measurements. The procedure was similar to that presented in detail elsewhere.[15,16] Before scratching, an initial surface profile of the samples was detected by pre-scanning the surface with the indenter under a low load of 100 μN. Depths of scratches with increasing scratch length were measured *in situ* by profiling the surface of the film before, during and after the scratch event, resulting in a total length of the test of 975 μm while the scratch length was 838 μm long or less, applied to all samples containing 5, 10, 15, 20, 25 and 30 wt-%TEOS. The normal load of indenter was linearly ramped from the minimum to the maximum (20 mN) during the scratching. The translation speed was typically 50 μm s^{-1}. After scratching, the surface of the samples was also examined by an optical microscope.

Results and discussion

Hardness and elastic modulus

The local values of hardness and elastic modulus of GST films modified with 5–30 wt-%TEOS (the films are denoted $F_{5\%}$–$F_{30\%}$, respectively) as a function of the penetration are shown in Fig. 1. The hardness profiles for GST coatings (soft-film/hard-substrate) can be divided into four regions (or layers): a superficial region, a region of maximum value, a region of constant value and a region showing a substrate effect.[21] Close to the surface (the first and second regions), a peak in mechanical properties may be recorded due to the pile-up effect.[26,27] There is also an effect of the substrate on load-displacement data when the indentation depth exceeds more than about 10% of the film thickness (the fourth region).[28,29] The third region is a limited one where intrinsic hardness of the coating may be determined.[21] The $F_{30\%}$ has the maximum average hardness, 0·33 GPa, measured in the limited range of 146–365 nm, because of the formation of harder structures containing more SiO_2 causing an increase in rigidity. For the plot of elastic modulus versus displacement, there is a small pile-up effect close to the surface, a very short plateau and a strong effect of the substrate, evidenced at very small penetrations. The influence of the substrate on the modulus measurement (elastic behaviour) is much stronger than that on the hardness determination (elastoplastic behaviour).[30] The $F_{20\%}$ has the maximum average modulus, 3·05 GPa, taken from the limited range of about 60–170 nm.

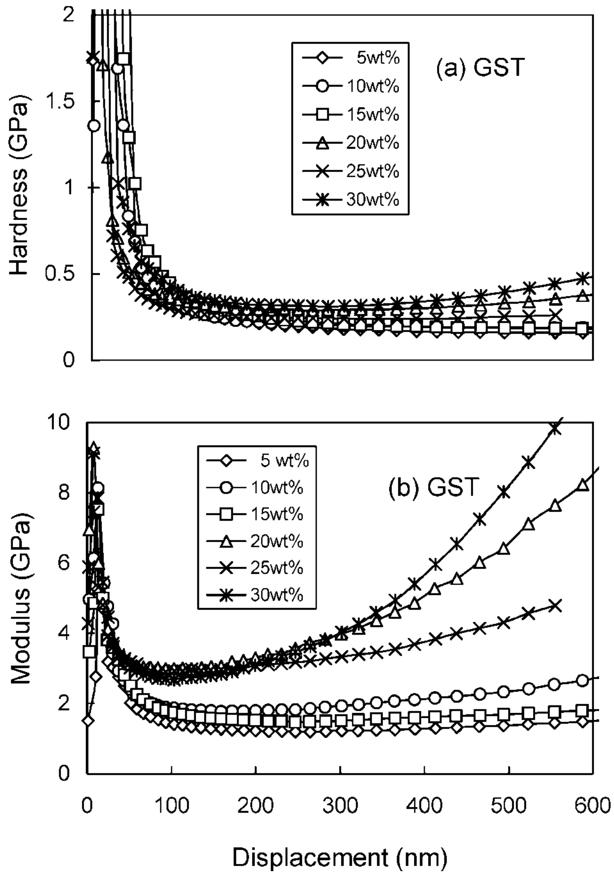

1 Effect of varying TEOS contents on *a* hardness and *b* elastic modulus of three GST coatings

Figure 2 shows the plots of the average values of hardness and elastic modulus versus the fractions of TEOS modifier. It is clear that the average values of hardness and elastic modulus increase with the increase in the content of TEOS. The hardness values greatly increase from 5 to 20% TEOS at the beginning because TEOS forms harder structures containing SiO_2 causing an increase in the rigidity of the systems[28] and the values slowly increase after 20% TEOS content, ascribed to the increase in TEOS content leading to a loose structure in the GST film.[31] Table 1 lists the hardness, elastic modulus and brittle index of GST containing different amounts of TEOS. It can be seen that the brittle index of $F_{20\%}$ is relatively low, despite its hardness approaching that of $F_{30\%}$.

Scratch profiles

Fig. 3 shows the scratch profiles of modified GST films with a ramping load of 0–20 mN during the pre-scan,

Table 1 Hardness, elastic modulus and brittle index of GST coatings containing varying amounts of TEOS

	GST		
TEOS, wt-%	Hardness, GPa	Elastic modulus, GPa	Brittle index (*H*/*E*)
5	0·15	1·30	0·115
10	0·20	1·80	0·111
15	0·18	1·67	0·108
20	0·29	3·05	0·095
25	0·24	2·89	0·083
30	0·33	2·74	0·120

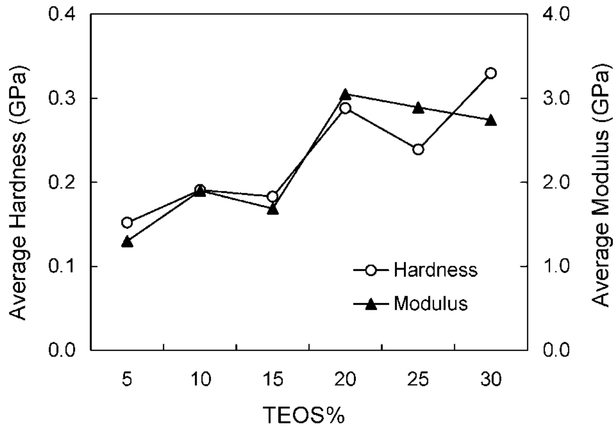

2 Average hardness and elastic modulus of three GST coatings as a function of TEOS content

scratch-scan and post-scan of the scratch testing. The pre-scan profiles the pre-scratched surface of GST films and the post-scan is used to assess the surface damage and the elastic/plastic deformation caused by the scratch event. The negative depth corresponds to a displacement of the scratch tip being pushed into the specimen, and the positive depth indicates the outward blistering of the surface or the accumulation of debris in the scratch test.[16] The effect of the various TEOS contents in the films on the scratch profiles is clearly observed in Fig. 3.

For the scratch profile of $F_{5\%}$ as seen in Fig. 3a, the pre-scan profiles a straight baseline, indicating that the surface of $F_{5\%}$ is extremely smooth. During the scratch ramping, the scratch tip can easily penetrate the surface layer and result in the highest vertical displacement, about 6·5 μm with 825 μm horizontal displacement, implying poorer hardness or scratch resistance. This also results in a large friction force at the beginning of the scratch and an increase in the coefficient of friction from 0 to 0·62 under a loading 0–0·70 mN, as shown in Fig. 4. The presence of fluctuations in the post-scan profile beneath the curve of the pre-scan implies that the film delaminates after unloading.[15] This is due to the smaller fraction of TEOS in $F_{5\%}$ and the formation of an inhomogeneous structure. However, there is no abrupt change in the scratching curve, implying that $F_{5\%}$ did not peel off during the scratch testing.[15] The scratch optical image for $F_{5\%}$ is illustrated in Fig. 5a. The scratch profiles of $F_{10\%}$ and $F_{15\%}$ as seen in Fig. 3b and c, are similar. The vertical displacements from their profiles are shorter than that of $F_{5\%}$, at about 3·8 μm and 3·4 μm for horizontal displacements of 703 μm and 838 μm, respectively, ascribed to the increase in hardness or scratch resistance with increasing amount of TEOS. This is in agreement with the profile shown in Fig. 2. The post-scan profiles of $F_{10\%}$ and $F_{15\%}$ are different from that of $F_{5\%}$, lying above the curve of the pre-scans, which indicates the outward blistering of the surface after unloading and the accumulation of debris in the scratch test, illustrated by the optical images in Fig. 5b and c.

For the scratch profiles of $F_{20\%}$ in Fig. 3d, the same pre-scan profile like that of $F_{5\%}$ is shown, also indicating the extremely smooth surface. The scratch-scan profile only goes down to a depth of about 2·7 μm corresponding to a horizontal displacement of 838 μm, the shortest depth among the films. This indicates the best

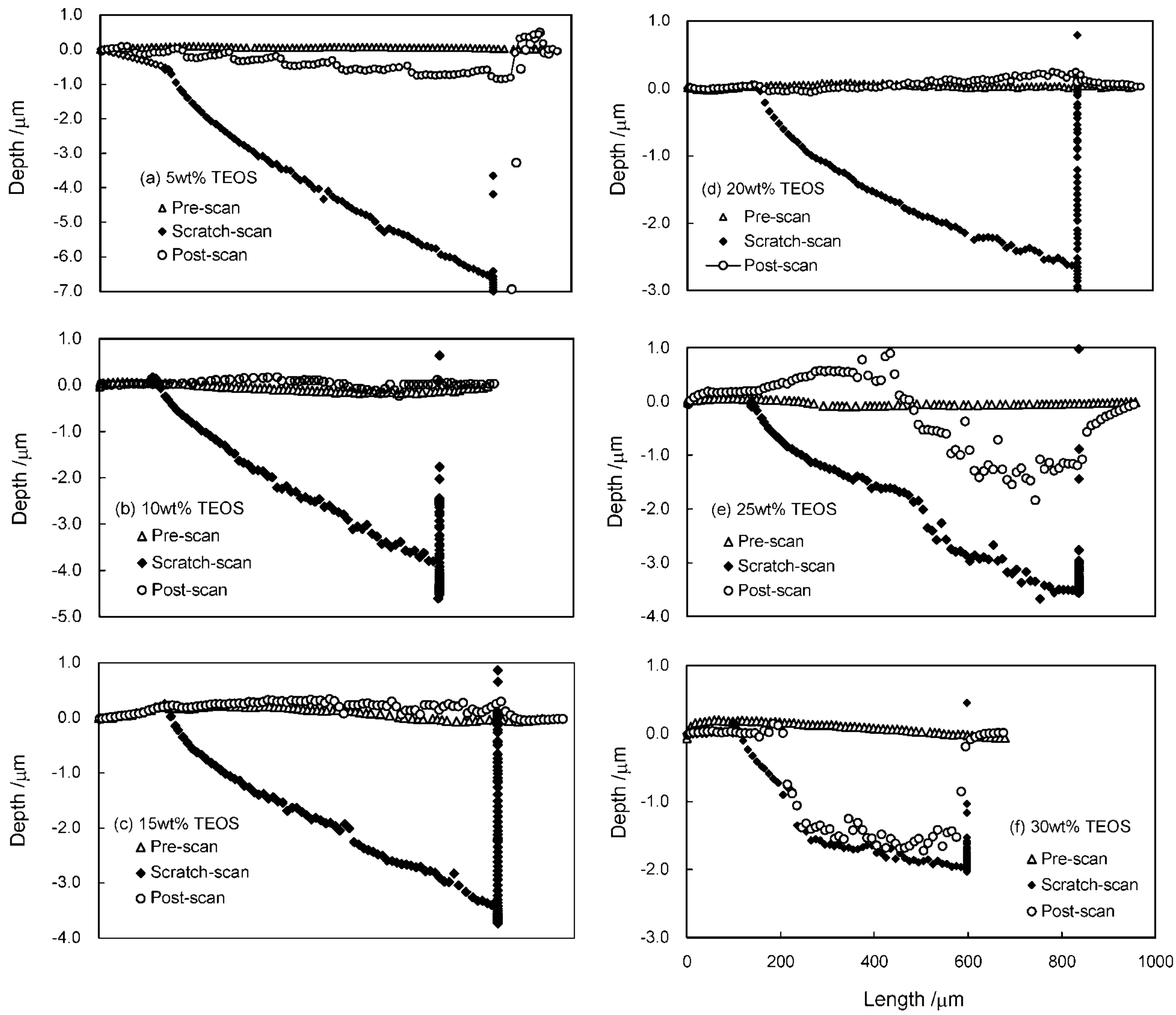

3 Scratch-testing profiles (pre-scan, scratch-scan and post-scan) of GST films with varying TEOS contents (wt-%): *a* 5, *b* 10, *c* 15, *d* 20, *e* 25 and *f* 30

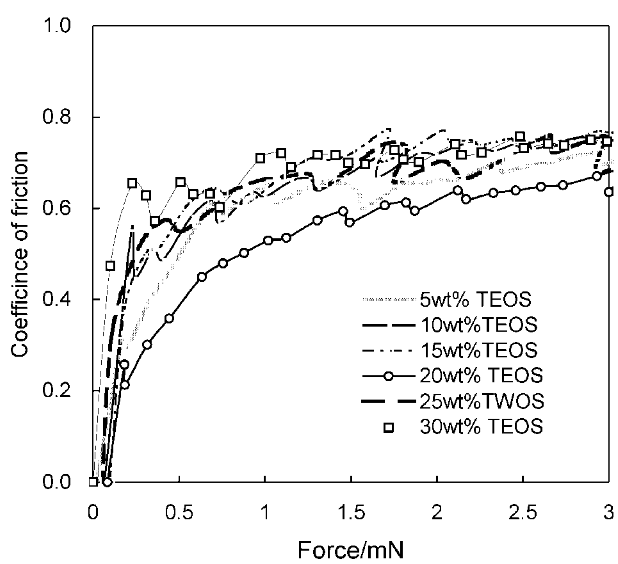

4 Coefficient of friction of GST films with varying TEOS contents (5, 10, 15, 20, 25 and 30 wt-%) as a function of scratch load

mechanical property (scratch resistance) of $F_{20\%}$ because of the adequate amount of TEOS in the modified system. There is no abrupt change in the scratching curve, i.e. $F_{20\%}$ was not peeled off during the scratch testing. The post-scan profile nearly coincides with the pre-scan baseline, showing that $F_{20\%}$ shows the best recovery among the films, and plastic deformation successively occurred with increasing normal load during scratching. The absence of fluctuations in the post-scan profile implies that $F_{20\%}$ did not delaminate after unloading, but showed a good adhesion. From Fig. 4, the friction coefficient of $F_{20\%}$ is lowest. There are some cracks along one side of the scratch trace in Fig. 5d, corresponding to the post-scan profile at a length of 600–838 μm in Fig. 3d.

The three-step profiles for $F_{25\%}$ and $F_{30\%}$ are different from the other four (Fig. 3) because of the undesirable microstructure. The pre-scan profile of $F_{30\%}$ is located above a horizontal baseline of zero. This is the result of more modifiers making the structure brittle and the surface rough and gives the largest coefficient of friction (0·65 under a loading of 0–0·23 mN) as seen in Fig. 4. The post-scan profile of $F_{25\%}$ and $F_{30\%}$ definitely cannot coincide with the pre-scan at any range of horizontal displacement, thus displaying the worst elastoplastic

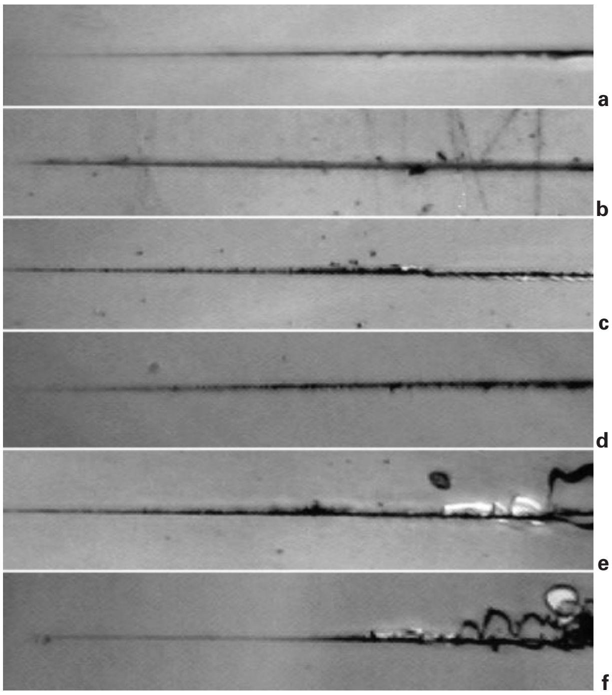

5 Optical images of scratch damage to GST films with varying TEOS contents (wt-%): *a* 5, *b* 10, *c* 15, *d* 20, *e* 25 and *f* 30

behaviour. There are some abrupt changes in the displacement curves of both the post-scan and the scratch-scan, demonstrating that $F_{25\%}$ and $F_{30\%}$ were seriously damaged by the ploughing and peeling off during the scratch testing,[15,16] which happened at the end of scratch trace as observed in Fig. 5e and f, displaying the worst scratch-resistance behaviour. More debris is found at the sides of the scratch tracks on $F_{25\%}$ and $F_{30\%}$, believed to be the result of particles pulled out during scratching, because of the high brittle index. In addition, it is indicated that the scratch traces of $F_{25\%}$ and $F_{30\%}$ are absolutely not smooth and shallow, as revealed in the optical images of Fig. 5e and f.

Conclusions

SSO derived from the hydrolytic condensation of GPMS and TEOS can be prepared by the sol–gel process, and the hardness and elastic modulus of GST films on glass substrates may be measured by the CSM technique to find the brittle index. The brittle index of $F_{20\%}$ is relatively low compared with the other layers (other than $F_{25\%}$), even though its hardness approached that of $F_{30\%}$, due to the different amount of TEOS added to make their microstructures different. The scratch-testing profiles of the films, including the pre-scan, scratch-scan and post-scan, were obviously influenced by varying the TEOS contents. For $F_{5\%}$, the poorer hardness, scratch resistance, plasticity and higher coefficient of friction shown in the scratch-testing profiles, was ascribed to the lower amount of TEOS in $F_{5\%}$ and the increased difficulty in retaining the initial state. The mechanical properties (hardness, modulus and scratch resistance) of $F_{10\%}$ and $F_{15\%}$ were much better than those of $F_{5\%}$. For $F_{25\%}$ and $F_{30\%}$, the higher hardness but lower elasticity, plasticity and scratch resistance and the highest coefficient of friction shown in the scratch-testing profiles, was ascribed to the higher amount of TEOS added to the film to form the rigid and loose structure. For $F_{20\%}$, the best plastic properties, elastic recovery and scratch resistance, and the lowest coefficient of friction shown in the scratch-testing profiles, was ascribed to the adequate amount of TEOS in the modified $F_{20\%}$, that makes it suitable and more effective as a protective coating.

Acknowledgements

Financial support is acknowledged from The Department of Science and Technology, The Government of Heilongjiang Province, China, under the contract numbers of WB02104 and GB1A2060.

References

1. J. D. Lichtenhan: in 'Organic/Inorganic Hybrid Materials', (ed. F. D. Blum & R. M. Laine), 17–41, 2003; USA, Division of Polymer Chemistry, Inc., ACS.
2. L. T. Metroke, O. Kachurina and E. T. Knobbe: *Prog. Org. Coat.*, 2002, **44**, 295–305.
3. B. Arkles: *MRS Bull.*, 2001, **26**(5), 402–407.
4. W. C. Oliver and G. M. Pharr: *J. Mater. Res.*, 1992, **7**(6), 1564–1583.
5. X. Li and B. Bhushan: *Mater. Charact.*, 2002, **48**, 11–36.
6. S. Sundararajan and B. Bhushan: *J. Mater. Res.*, 2001, **16**(2), 437–445.
7. A. Dasari, J. Rohrmann and R. D. K. Misra: *Mater. Sci. Eng.*, 2003, **A354**, 67–81.
8. M. P. de Boer, J. C. Nelson and W. W. Gerberich: *J. Mater. Res.*, 1998, **13**(4), 1002–1013.
9. F. Davanloo, C. B. Collins and K. J. Koivusaari: *J. Mater. Res.*, 1999, **14**(8), 3474–3482.
10. X. Li, B. Bhushan and M. Inoue: *Wear*, 2001, **251**, 1150–1158.
11. L. Huang, K. Xu and J. Lu: *Diam. Rel. Mater.*, 2002, **11**, 1505–1510.
12. B. Bhushan and X. Li: *J. Mater. Res.*, 1997, **12**, 54–63.
13. B. Bhushan, B. K. Gupta and M. H. Azarian: *Wear*, 1995, 181–183, 743–758.
14. S. Roche, S. Pavan, J. L. Loubet, Ph. Barbeau and B. Magny: *Prog. Org. Coat.*, 2003, **47**, 37–48.
15. C. Charitidis, Y. Panayiotatos and S. Logothetidis: *Diam. Relat. Mater.*, 2003, **12**, 1088–1092.
16. L. Huang, K. Xu, J. Lu, B. Guelorget and H. Chen: *Diam. Rel. Mater.*, 2001, **10**, 1448–1456.
17. L. Huang, K. Xu, and J. Lu: *Diam. Rel. Mater.*, 2002, **11**, 1505–1510.
18. P. Lemoine, J. F. Zhao, J. P. Quinn, A. A. Ogwu, J. A. McLaughlin, P. Maguire, F. McGinnity and X. Shi: *Wear*, 2000, **244**, 79–84.
19. N. Tayebi, T. F. Conry and A. A. Polycarpou: *J. Mater. Res.*, 2003, **18**(9), 2150–2162.
20. C. J. Buchko, M. J. Slattery, K. M. Kozloff, D. C. Martin: *J. Mater. Res.*, 2000, **15**(1), 231–242.
21. L. Hu, X. Zhang, H. You, Y. Liu, H. Zhang and D. Sun: *J. Mater. Sci.*, 2004, **39**, 1331–1335.
22. P. Innocenzi, M. Esposto and A. Maddalena: *J. Sol–Gel Sci. Tech.*, 2001, 20(3), 293–301.
23. J. D. Mackenzie and E. P. Bescher: *J. Sol–Gel Sci. Tech.*, 2000, **19**, 23–29.
24. P. Eisenberg, R. Erra-Balsells, Y. Ishikawa, J. C. Lucas, H. Nonami and R. J. J. Williams: *Macromolecules*, 2002, **35**, 1160–1168.
25. J. Malzbender, J. M. J. den Toonder, A. R. Balkenende and G. de With: *Mater. Sci. Eng.*, 2002, **36**, 47–103.
26. T. Y. Tsui, W. C. Oliver and G. M. Pharr: *Mater. Res. Soc. Symp. Proc.*, 1997, **436**, 207–212.
27. R. Saha and W. D. Nix: *Mater. Sci. Eng.*, 2001, **A319–321**, 898–901.
28. T. Y. Tsui, C. A. Ross and G. M. Pharr: *Mater. Res. Soc. Symp. Proc.*, 1997, 436, 57–62.
29. J. Kim, D. Kim and P. Hwang: *J. Mater. Sci.*, 2000, 35, 4185–4192.
30. M. Tabbal, P. Mérel, M. Chaker, M. A. El Khakani, E. G. Herbert, B. N. Lucas and M. E. O'Hern: *Surf. Coat. Technol.*, 1999, **116–119**, 452–455.
31. L. Hu, Z. Lu, X. Zhang, D. Sun and Y. Huang: *PMSE Prep.*, 2003, **88**, 193–194.